NOAA Technical Memorandum ERL PMEL-12

A SHALLOW WATER PRESSURE-TEMPERATURE GAGE (PTG): DESIGN, CALIBRATION, AND OPERATION

Stanley P. Hayes
John Glenn
Nancy N. Soriede

Pacific Marine Environmental Laboratory
Seattle, Washington
June 1978

UNITED STATES DEPARTMENT OF COMMERCE
Juanita M. Kreps, Secretary

NATIONAL OCEANIC AND ATMOSPHERIC ADMINISTRATION
Richard A. Frank, Administrator

Environmental Research Laboratories
Wilmot N. Hess, Director

DISCLAIMER

The NOAA Environmental Research Laboratories does not approve, recommend, or endorse any proprietary product or proprietary material mentioned in this publication. No reference shall be made to the NOAA Environmental Research Laboratories, or to this publication furnished by the NOAA Environmental Research Laboratories, in any advertising or sales promotion which would indicate or imply that the NOAA Environmental Research Laboratories approves, recommends, or endorses any proprietary product or proprietary material mentioned herein, or which has as its purpose an intent to cause directly or indirectly the advertised product to be used or purchased because of this NOAA Environmental Research Laboratories publication.

CONTENTS

FIGURE CAPTIONS

A SHALLOW WATER PRESSURE-TEMPERATURE GAGE (PTG): DESIGN, CALIBRATION, AND OPERATION

Stanley P. Hayes
John Glenn
Nancy N. Soriede

An internally recording, low power instrument to measure water pressure and temperature in water depths of up to 250 m is described; calibration and processing techniques are discussed; some field results are presented. The gage uses a quartz crystal pressure transducer, an epoxy-coated thermistor, and a commercially available digital recording system. Calibration results show a temperature dependence which can amount to 1 mb/°C for some gages at some pressures. This is a combined effect due to the temperature dependence of the clock and of the pressure transducer. Long-term drift of the pressure transducer could not be accurately assessed by the laboratory tests, but appeared to be roughly of the same magnitude as the manufacturer's specification for the transducer. Results from deployments in the Gulf of Alaska showed six month records which had trends of less than 1 cm/mo. Much of this trend could be oceanic.

1. INTRODUCTION

In fall 1974, the Pacific Marine Environmental Laboratory initiated a research program to investigate the currents on the continental shelf in the Gulf of Alaska and their response to wind forcing. Of particular interest was precision measurement of the pressure field at the ocean bottom, in order that fluctuations in pressure gradient across and along the continental shelf could be correlated with the currents. These pressure gradient fluctuations, which are caused by a variety of mechanisms (tidal and nontidal) are important in the dynamics of ocean circulation. Preliminary calculations indicated that nontidal pressure changes of order 10 mb (1 mb is approximately equivalent to 1 cm of sea-level change) in 100 m of water would accompany a winter storm. This signal level set requirements on the pressure gage. Its resolution had to be at least .01% in order to resolve the fluctuations, and any low-frequency drift had to be small compared to .01% over the time period of the storm-induced currents (of order 1 week).

A survey of the available pressure transducers and recording systems at that time indicated that the Digiquartz Model 2400A quartz crystal pressure transducer manufactured by Paroscientific Incorporated, Redmond, Washington, was ideal for our applications. A commercial pressure gage (model TG-2A) manufactured by Aanderaa Instruments Ltd., Victoria, Cana-

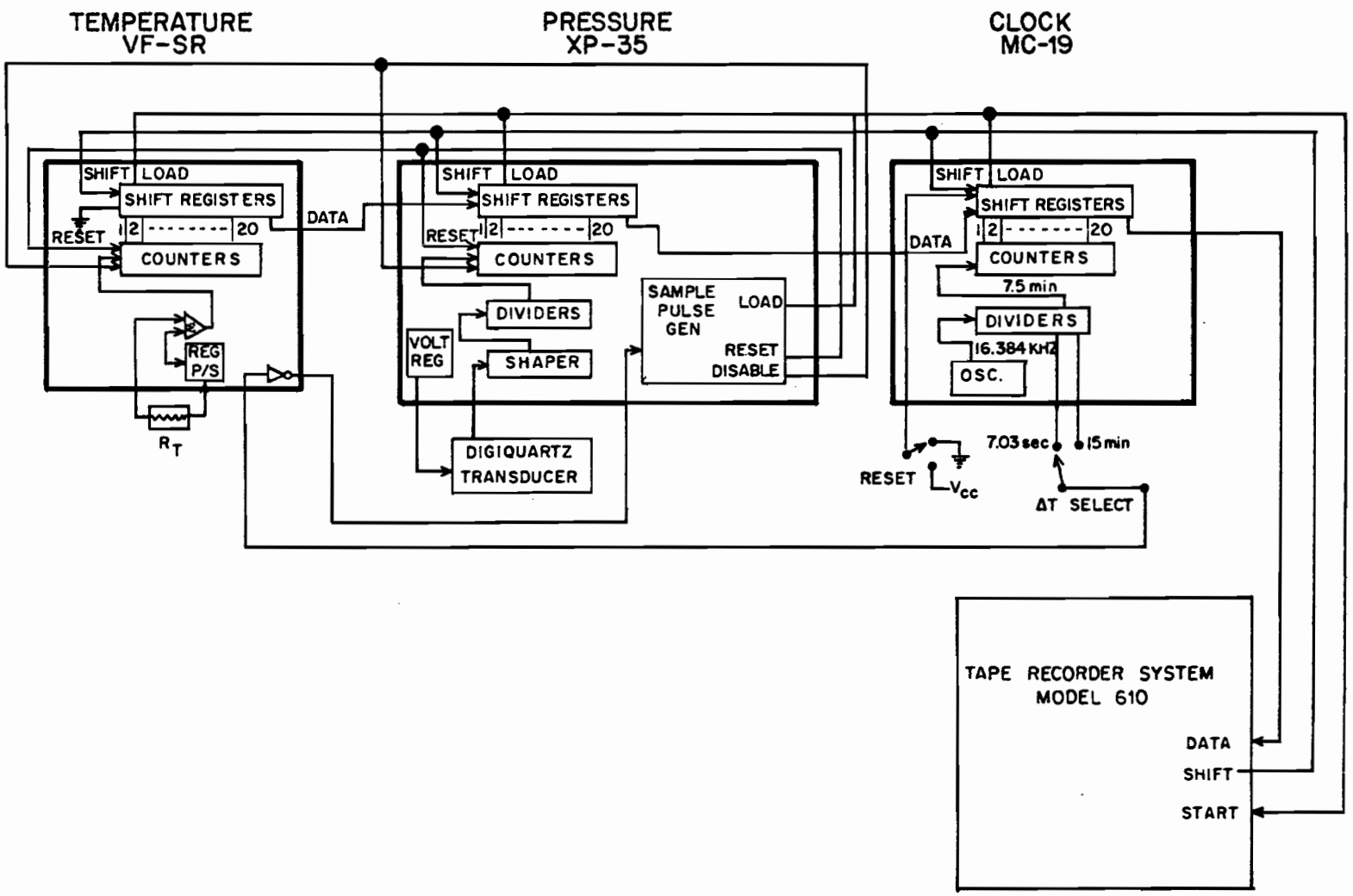

Figure 1. Block diagram of electronics.

da, which used the Digiquartz sensor was available in 1974. We chose not to utilize this gage since it did not record time or temperature on the magnetic tape. Instead, a pressure-temperature gage (PTG) was designed which utilized a Digiquartz pressure transducer, a thermistor bead, model 44032, made by Yellow Springs Instrument Company, Yellow Springs, Ohio, and a Sea Data recording system manufactured by Sea Data Corporation, Newton, Massachusetts. Pressure measuring systems similar to the one discussed here have been developed in several laboratories. A particular system has been described by Culverhouse (1977). Rather than repeat the details which can be found elsewhere, we will present the general operating characteristics of the PTG with emphasis on its distinctive features. The system calibration, processing techniques, and several results will then be discussed.

2. INSTRUMENT DESIGN

2.1 Sensors

2.1.1 Pressure

The instrument utilizes the model 2400A Digiquartz pressure transducer mounted in a model 300 shock mount. Full information on this transducer is available from the manufacturer and in the article by Paros (1976). In brief, the transducer is a quartz crystal oscillator with a frequency which varies with applied pressure. The nominal frequency range is 40 kHz (0 psia) to 36 kHz (400 psia). The transducer requires low power (about 800 μA). The manufacturer specifies a long-term drift rate of better than .01% per year. The transducer is connected to the ocean via an oil-filled nylon tube. The tube and transducer are filled with Dow Corning silicone oil using a vacuum technique. The oil is in direct contact with the seawater.

2.1.2 Temperature

The temperature measurements are made with a YSI model 44032 bead thermistor. These thermistors are calibrated in order to yield a precision of .01°C. The thermistor is mounted adjacent to the pressure transducer shock mount inside the PTG pressure case.

2.2 Electronics

A block diagram of the PTG electronics is shown in Figure 1. There are six printed circuit cards (all but the VFSR card are manufactured by Sea Data Corp.) The data is recorded by a Sea Data model 610 four-track digital recorder which consists of a model 64E tape transport, CR-12 motor driver card, CR-21 head driver card, and CR-30 cassette control card. The XP-35 pressure card, the VFSR temperature card, and the MC-19 clock card make up the remainder of the electronics. These components are described below.

2.2.1 Recording Sequence

The Sea Data digital cassette recording system records 18 characters during each recording sequence. The order of the data words on the tape is: two header characters, five characters (20 bits) of TIME data, six characters (24 bits) of PRESSURE data, and five characters (20 bits) of TEMPERATURE data.

The length of time that the pressure and temperature data are integrated is the $\Delta\tau$, preselected presently to be 7.03 s for calibration and 15 min during deployment. Therefore, during deployment the data are integrated (counts stored) for 15 minutes. The data are then recorded. The counts which may occur during the brief recording time are saved so that no count loss occurs.

A level change from the MC-19 clock card occurring at $\Delta\tau$ is sent to the XP-35 pressure card where the sample pulse generator generates three signals: LOAD, RESET, and DISABLE (Fig. 2).

The LOAD signal goes to the CR-30 cassette control card where it is seen as a RECORD REQUEST (START) and initializes the tape recording system.

The LOAD pulse also goes to the shift registers in the pressure, temerature, and clock processors. These registers will continue to follow the asynchronous parallel data bit inputs until the time when the LOAD pulse decays; then the inputs from the counter registers are jammed into the shift registers. At this time, RESET is generated which goes to all the count registers in the pressure and temperature processors, and the registers are all reset to Ø.

During this time, DISABLE inhibits any further counts from passing through the pressure and temperature memory gates.

SHIFT pulses generated by the CR-21 head driver card are then sent in parallel to all shift registers where the data bits are serially shifted through the registers to the CR-21 head driver PCB for recording. The serial bit train is configured into 4-bit parallel characters for recording. The most significant bits are recorded first.

2.2.2 Clock Card

The MC-19 clock card initiates the recording sequence at preset intervals. The oscillator output is adjusted to be 16.384 kHz (61.03516 μs period) at 6°C (the nominal deployment temperature). The MC-19 provides for several divisions of the basic clock frequency. In general we use 7.03-s and 900-s record intervals for calibration and deployment, respectively. The TIME word generated by the MC-19 was chosen to update every 7.5 min in order to be compatible with other instruments used in the laboratory.

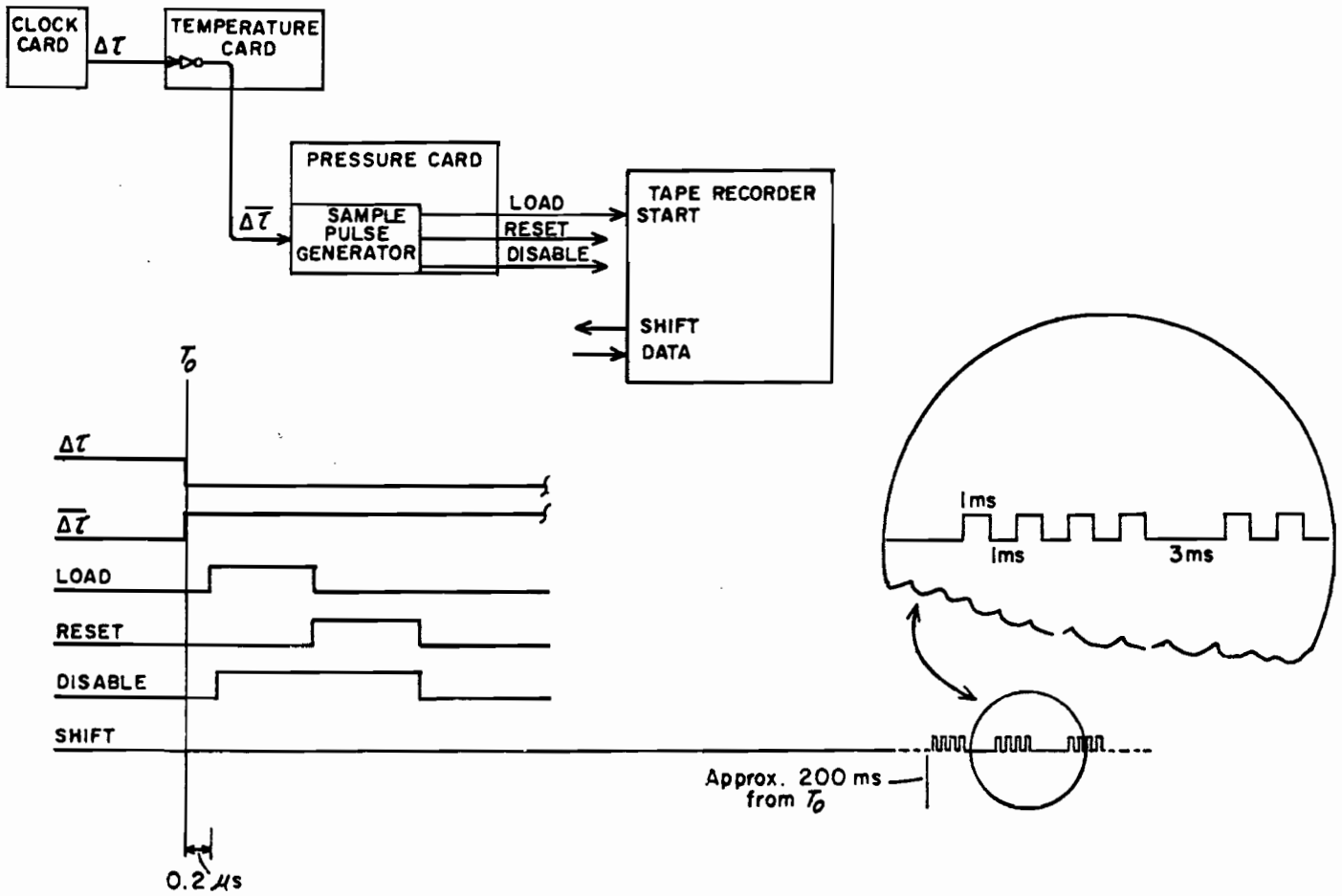

Figure 2. Timing Diagram.

2.2.3 Pressure Card

The XP-35 pressure card processes the signal from the Paroscientific transducer. This 3-V peak-to-peak square wave enters the XP-35 on pin 29, is shaped by a Schmitt trigger, and buffered prior to being prescaled by a factor of 4. The prescaled signal is counted, via a memory gate, by a 24-bit counter register for the integration period $\Delta\tau$.

At the end of the integration period, the record sequence is initiated; the counter registers are disabled from counting and their output is loaded into the data shift registers, the counter registers are reset, and the data bits are serially shifted to the tape recorder. The memory gate prevents a count loss during the brief LOAD-RESET-DISABLE portion of the recording sequence.

2.2.4 Temperature Card

The VFSR temperature processing card was developed in our laboratory by A. M. Zwilling. It combines the voltage to frequency conversion, the frequency counting, and the shift register onto a single card. The VFSR schematic diagram is in Figure 3. The thermistor, in series with a 3.9-V d.c. regulated voltage source, is applied across the input of an operational amplifier. The output of the amplifier is integrated to produce a linearly increasing voltage. When this integrated voltage reaches a preset value, a pulse is created; the integral is reset to zero by a negative voltage applied to the input of the amplifier. The frequency of pulses is a function of the resistance of the thermistor. At the end of the integration period, the recording sequence is initiated; then the events occur as described for the pressure word.

2.2.5 Power Supply

The PTG is powered by a five-tier battery pack having a total of 56 alkaline "D" cells (Mallory MN-1300). These cells are configured to provide three voltage levels. With this pack and a 15-min record cycle, the instrument is capable of a year-long deployment.

2.3 Mechanical Structure

The PTG is housed in a 32-in shallow water pressure case manufactured by AMF, Alexandria, Virginia (part no. 11104). The endcaps for the pressure case (AMF part no. 11105) require some modifications for the pressure port in the upper end cap and for cathodic protection.

The frame for mounting the printed circuit boards, the cassette recorder, battery pack, and pressure transducer is similar to the design used in the AMF VACM (Vector Averaging Current Meter). In the PTG, sufficient space is available for two additional printed circuit boards if other sensors are required.

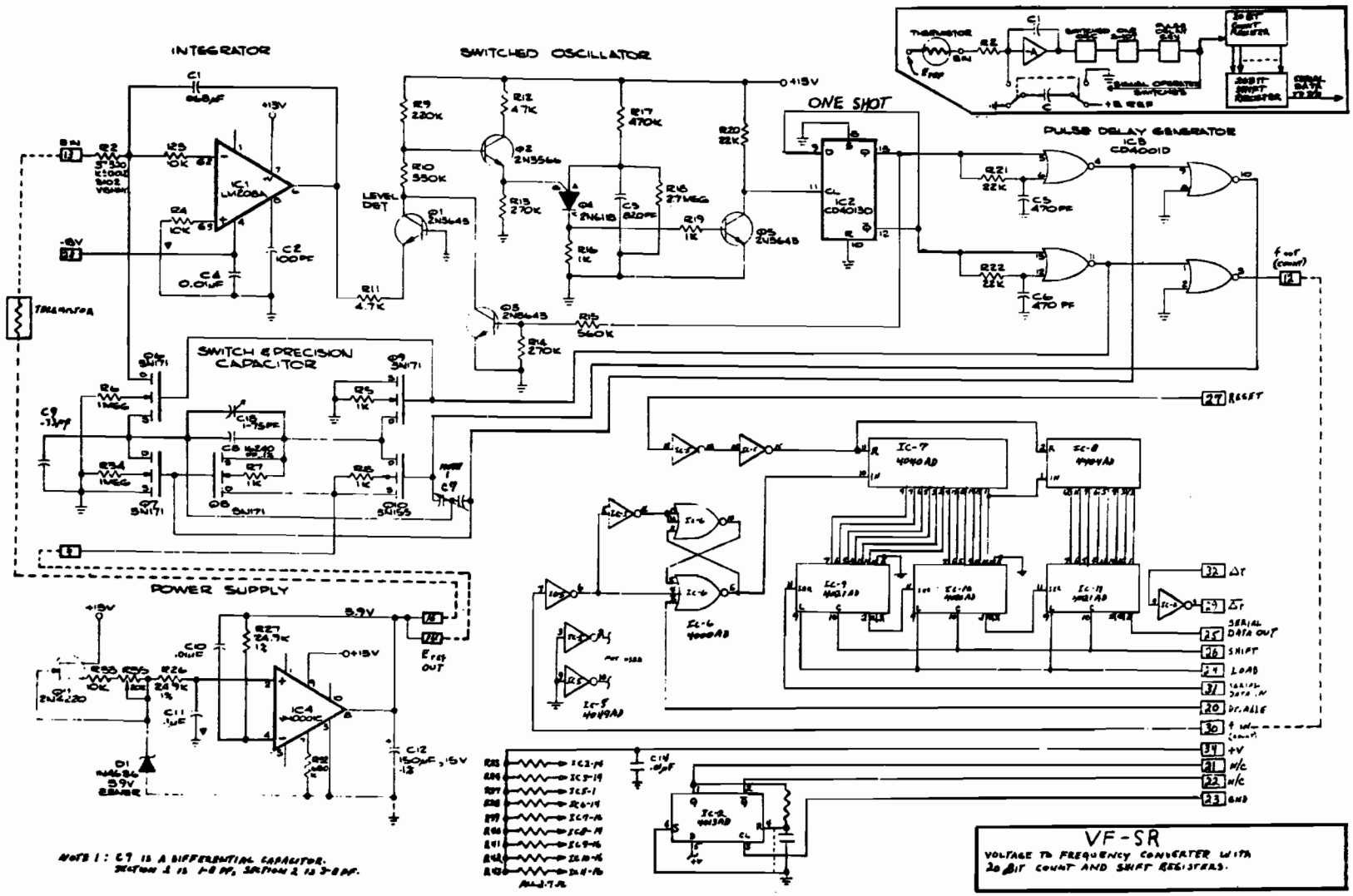

Figure 3. Schematic diagram of the VFSR temperature interface card.

3. CALIBRATION

The PTG instruments are calibrated to obtain the conversion equations for pressure and temperature. Since both the clock and the pressure transducers employ quartz crystal oscillators, we expect a temperature dependence to the calibration. Considering first the clock, the manufacturer (Sea Data Corp.) specifies a temperature dependence as shown in Figure 4 for the MC-19. The dependence found by Culverhouse (1977) was somewhat greater (approximately 16 ppm between 14°C and 4°C). For our work in the Gulf of Alaska, ambient temperature is normally between 3°C and 10°C. Thus, if the clock were set at room temperature, we would expect time errors of order 15 ppm. This error would yield an apparent clock drift of about 10 minutes per year. In some applications, this drift might be significant. To reduce the drift, the clock period is set to be 61.02516 μs at 6°C. The temperature dependence (about 2 ppm/°C) is still present; however, the net effect is reduced. Observed clock drifts based on pre- and post-deployment clock checks are generally less than 2 minutes in 6 months.

The temperature dependence of the clock also affects the measured pressure. Since the number recorded on the cassette tape is counts per time interval, the varying clock period affects the recording interval and, hence, the apparent pressure. Assuming a 2 ppm/°C clock temperature dependence, the error in recorded pressure would be about 0.6 mb/°C. This clock-induced temperature dependence is in addition to the temperature dependence of the digiquartz transducer. From manufacturer specifications, the digiquartz pressure sensor temperature dependence varies with applied pressure. A maximum temperature dependence of about 1 mb/°C is possible. If uncorrected, the total temperature dependence would seriously degrade the precision of the gage. Therefore, the gages were calibrated at three temperatures, as described below. Since the entire gage was immersed in the temperature bath, both the clock and the pressure sensor temperature dependences are combined in the final calibration curves.

3.1 Pressure

The pressure response of the PTG is calibrated at Northwest Regional Calibration Center (NWRCC), Bellevue, Washington. In most cases, several gages are calibrated simultaneously; this provides a consistency check on the pressure source. The gages are calibrated at three temperatures which span the temperature range expected during deployment. Nominally, 3°C, 5°C, and 8°C are used for Alaskan deployments. Prior to calibration, the recording interval is set to 7.03 s, the clock reset time is carefully noted, and the gages are packaged in the pressure cases. At NWRCC the PTG is immersed in a temperature bath and allowed to stabilize for at least 1 hour.

All gages being calibrated are connected through a manifold to the pressure control panel of an air piston gage. Pressure is applied in nominal 40 psia (1 psia = .689 mb) increments from 0 to 400 psia. The exact pressure at each point is determined by the calibrated piston area and the

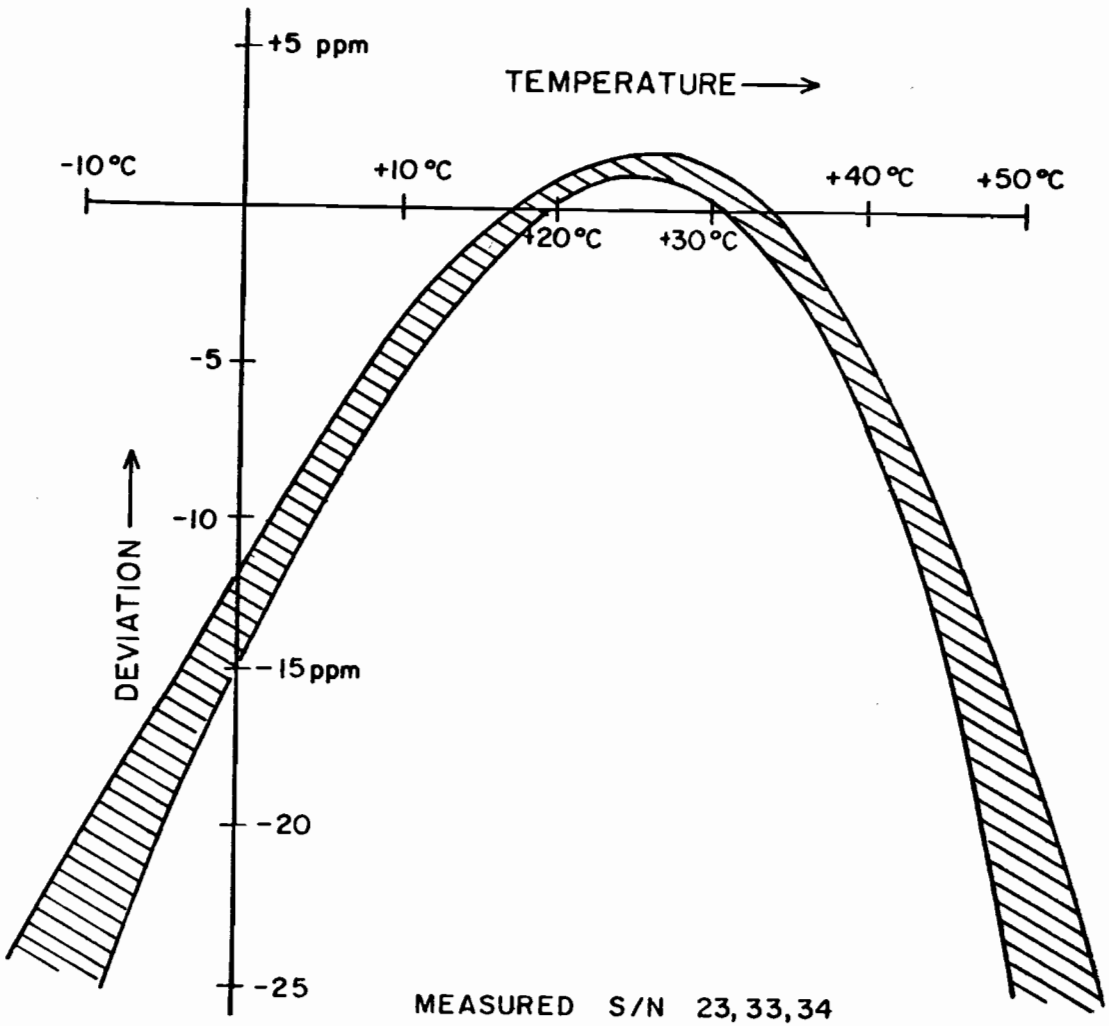

Figure 4. Manufacturer's specification for temperature dependence of MC-19 clock card.

mass of the weights used at each pressure. Corrections are made for the effect of heat, gravity, the temperature effect on the piston assembly, and the height difference between the pressure tester reference and the instrument pressure port. An estimate of the uncertainty of each pressure value is given, based on uncertainties in the above quantities. The accuracy of the pressure value varies from .003 psia at 40 psia to .03 psia at 400 psia.

For the zero pressure point, the sensor is connected to a vacuum pump and the vacuum is monitored using a thermocouple vacuum gage. For other pressure points, the air piston gage is sealed with a bell jar which is evacuated to a maximum of 100 μm. The pressure manifold is slowly charged with dry nitrogen until the piston, weighted with the appropriate mass, floats on the nitrogen. The pressure control panel is then adjusted to keep the piston balanced at a reference point for 2 minutes. This allows for about 17 samples at the 7.03-s record interval. The time for each pressure point is recorded for later comparison with the data tape.

3.1.1 Pressure Calibration Algorithm

The number recorded on the cassette represents the counts observed during the integration time $\Delta\tau$. These counts have been scaled by a factor of 4 prior to recording. Since the calibration equation is in terms of frequency, the counts are first converted to frequency.

For each temperature, a least squares fit is used to determine the coefficients of a third order polynomial,

$$p = a_0 + a_1 f + a_2 f^2 + a_3 f^3, \qquad (1)$$

where p is the applied pressure and f is the frequency recorded by the PTG at the applied pressure. In determining f from the cassette tape, 10 values in the center of the 2-minute interval with constant pressure p are used. Each 7.03-s sample has a frequency uncertainty of 0.57 Hz (4 counts/$\Delta\tau$). The use of 10 samples reduces this uncertainty to .057 Hz which corresponds to about 0.4 mb in pressure.

The third order frequency calibration was used rather than the second order polynomial suggested by the National Bureau of Standards (see Culverhouse, 1977) since the calibration we perform is actually a combined clock and pressure transducer calibration. Figure 5 shows a comparison of the residuals obtained with a second and third order fit. Figure 6 shows the typical residuals obtained. Maximum residuals are about 0.05 psia (3 mb). Further discussion of calibration results are in section 3.3.

The temperature dependence of the pressure calibration is shown in Figure 7, where the error introduced by using the 5°C calibration curve on data at 3°C and at 8°C is plotted. The magnitude of the error depends on pressure and is presented for 40, 160, and 360 psia.

A linear temperature dependence is included in the processing of the gages. An average frequency, f_a, is calculated for the deployment. Let

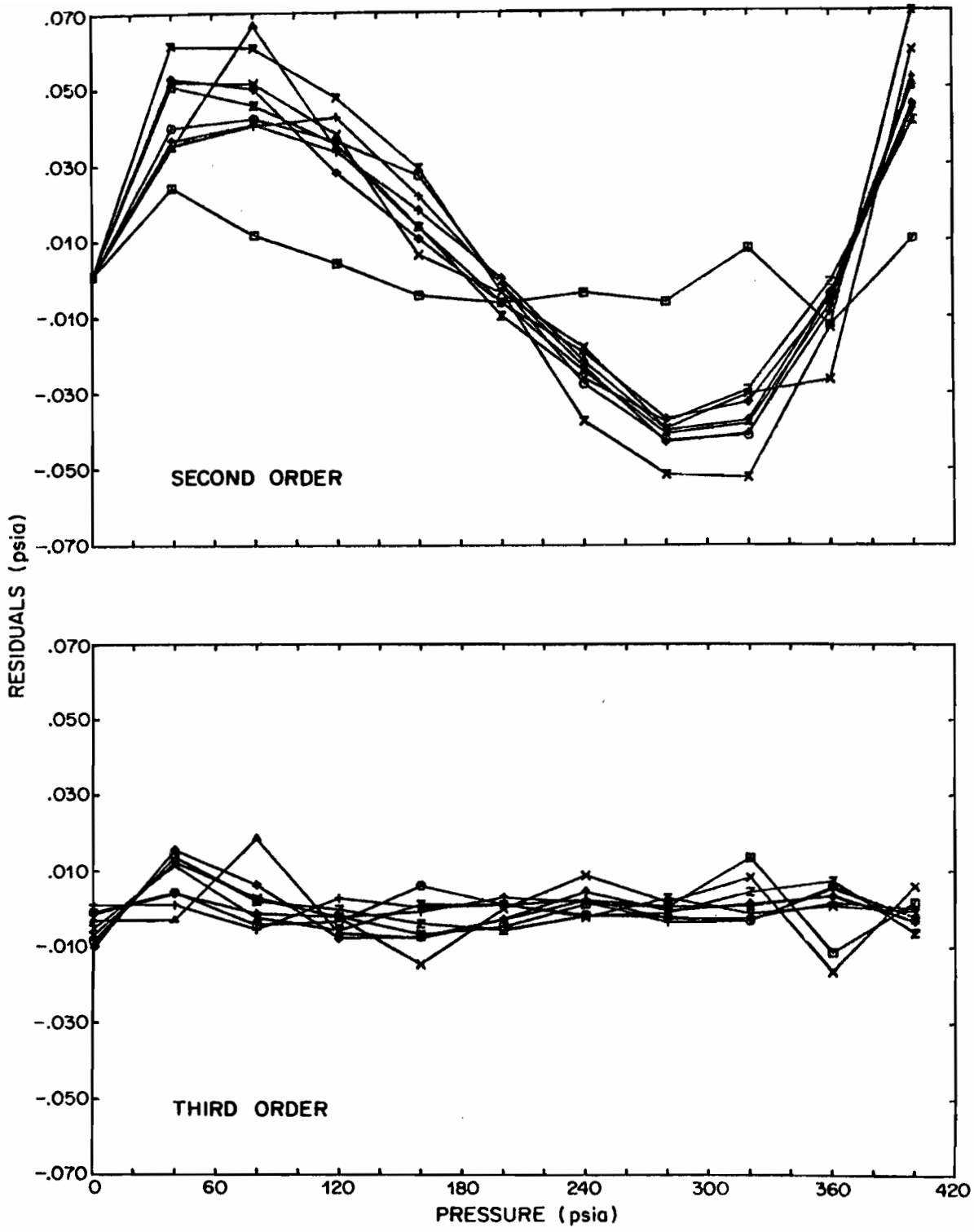

Figure 5. Residuals between applied and calculated pressure using a second- and third-order polynomial in frequency.

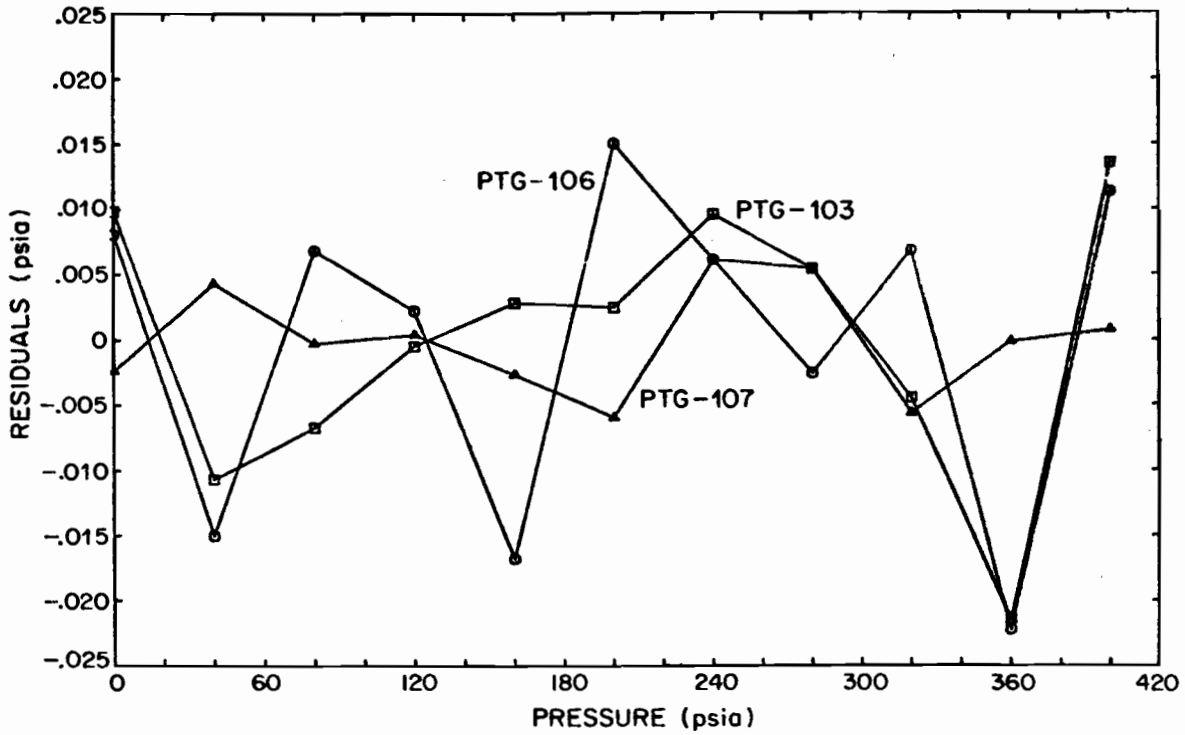

Figure 6. Typical residuals between applied and calculated pressure using a third-order polynomial in frequency.

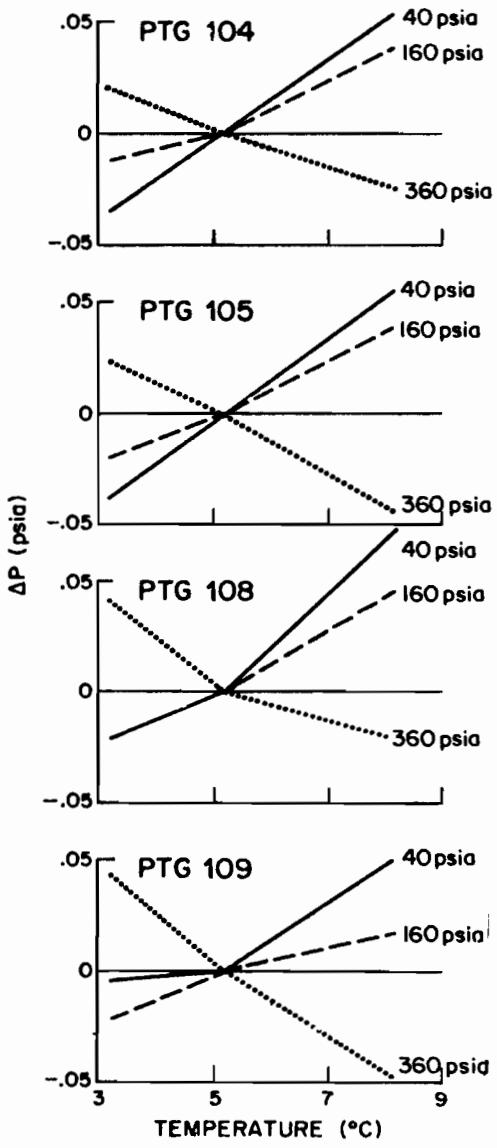

Figure 7. Temperature dependence of pressure gage for ambient pressure near 40, 160, 360 psia. The residual curves are shown for several gages.

p_3, p_5, and p_8 be the calibration polynomial determined for the gage at 3°, 5° and 8°C. Then if the recorded temperature, t, was less than 5°C, the pressure assigned to a frequency, f, is

$$p(f) = p_5(f) + \frac{p_5(f_a) - p_3(f_a)}{5. - 3.} \times (5 - t) . \qquad (2)$$

If $t > 5°C$, then

$$p(f) = p_5(f) + \frac{p_8(f_a) - p_5(f_a)}{8. - 5.} \times (t - 5) . \qquad (3)$$

The size of the temperature correction depends on the gage as indicated in Figure 8. Maximum temperature dependence occurs for high and low pressures with a coefficient of about .02 psia/°C (1 mb/°C).

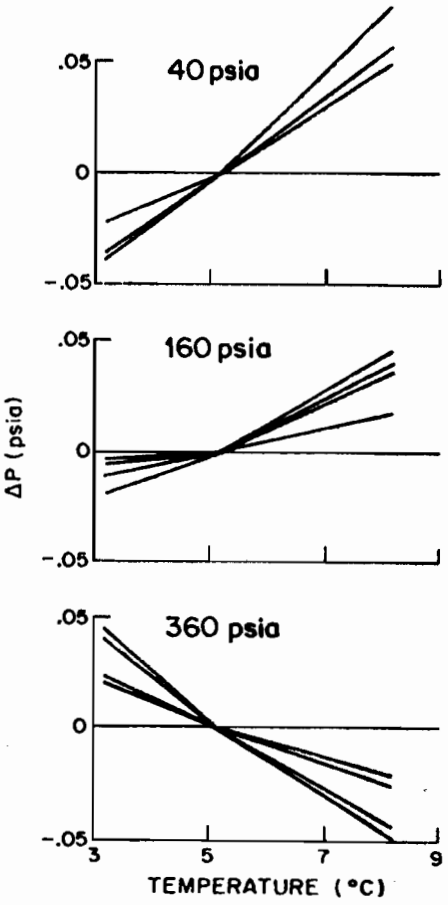

Figure 8. Gage dependence of the temperature effect. At each pressure the temperature correction is shown for the four gages included in Fig. 11.

3.2 Temperature Calibration

The temperature calibration consists of calibrating the thermistors to give resistance as a function of temperature and calibrating the temperature card (VFSR) to give output counts (frequency) as a function of resistance.

The thermistor calibration is performed at NWRCC. Calibration is at seven temperatures from 0°C to 30°C in 5°C increments. During most of the calibration period, the thermistors are powered (3.9 V d.c.) to simulate normal operating conditions with the accompanying self heating.

To measure the resistance, each thermistor is switched to a measuring bridge and the resistance is recorded. Temperature and resistance are related by the Steinhart-Hart equation (Steinhart and Hart, 1968),

$$T^{-1} = A + B \log_{10} R + C(\log_{10} R)^3 , \qquad (4)$$

where T = temperature, °K; R = resistance, ohms; and A, B, C = coefficients determined by a least squares fit to calibration data.

The temperature card (VFSR) is calibrated in the laboratory using a Vishay ohmic standard. The VFSR card is adjusted to a signal output period of 1820.4 μs with an input resistance of 74.440 κΩ. Measurements are then made with seven different input resistors, which correspond to nominal thermistor resistances for temperatures from 0°C to 30°C in 5°C increments. These resistances are 94.98, 74.44, 58.75, 46.67, 37.30, 30.00, and 24.27 κΩ. The card calibration is then given by a least squares linear regression of the measured period with the input resistance,

$$R = a_0 + a_{1_\tau} , \qquad (5)$$

where R is resistance, ohm; τ is period, seconds; and a_0 , a_1 are the regression coefficients.

3.3 Pressure Calibration Tests

In addition to the standard calibration procedures discussed in section 3.2, several of the gages have been subjected to special tests in order to study the effect of (a) long-term drift, (b) hysteresis, (c) flow past the sensor. In this section these tests are discussed and the results presented. Although in some cases the results were inconclusive, the problems observed may be of use to other investigators.

3.3.1 Long-term Drift

The drift rate of the Paroscientific transducer specified by the manufacturer is less than .01% of full scale per year. For the 400-psia transducer which we use, this translates into about 3 mb per year. The drift rate was established on the basis of repeated comparison between the

transducer and a standard. Unfortunately, our newly developed gages were immediately deployed in a field experiment, without time for detailed intercomparisons of long-term effects. To study these problems we relied on pre- and post-deployment calibrations and on the structure of the field data itself. Early results indicated that the gages were stable in terms of relative pressure fluctuations. That is, the derivative of the calibration curve, dP/df, at a given pressure, was constant with time. For the two gages PTG-100 and PTG-102, which were calibrated in March 1976 and February 1977, the change in $\Delta p/\Delta f$ was .01%. This small drift will not significantly affect the pressure determination.

To check for a slow drift in the absolute pressure measurement, pre- and post-deployment calibrations were considered. These did not yield a consistent pattern for any gage. There are several possible reasons for discrepancies between calibrations: the gage height relative to the pressure source, the clock frequency drift, pressure transducer hysteresis, pressure transducer drift. To investigate the validity of the absolute pressure determinations, we calibrated a gage, completely disconnected the gage from the pressure tester, reconnected it, and calibrated the gage again. The results shown in Figure 9 indicate that differences of order .025 psia (about 1.5 mb) occurred between the two tests. These differences are comparable to the pre- and post-deployment differences. The cause of the discrepancy has not been found, although pressure transducer hysteresis will contribute. At present we rely on the long-term trend observed in the data to set an upper limit on the transducer drift. This data is discussed in section 5.1.

3.3.2 Pressure Transducer Hysteresis.

Pressure gage hysteresis has been measured for several units. The calibration was first performed from 40 psia to 360 psia and then from 360 psia to 40 psia. Pressure to the gage was maintained while the weights were being changed. Results in Figure 10 show maximum hysteresis of about .06 psia (4 mb). Since the gage is subjected to nearly constant pressure ($\pm$ 3 psia) when it is deployed, the hysteresis is not considered important.

3.3.3 Bernoulli Effect

A decrease in pressure may result from flow around the sensor port. This dynamic pressure effect varies as

$$\Delta P = \tfrac{1}{2}\rho |v|^2 \quad . \tag{6}$$

A rough calculation predicts a pressure change of 5 mb for a 100 cm/s current. However, the geometry of the pressure port is important and the effect could vary significantly with instrument orientation. To check the importance of the Bernoulli effect, we towed a PTG in the U.S. Army Corps of Engineers Bonneville Test Facility. The instrument was vertical and towed horizontally (i.e. pressure port was perpendicular to flow) at speeds of 20 cm/s and 100 cm/s. At the low speed the pressure response was

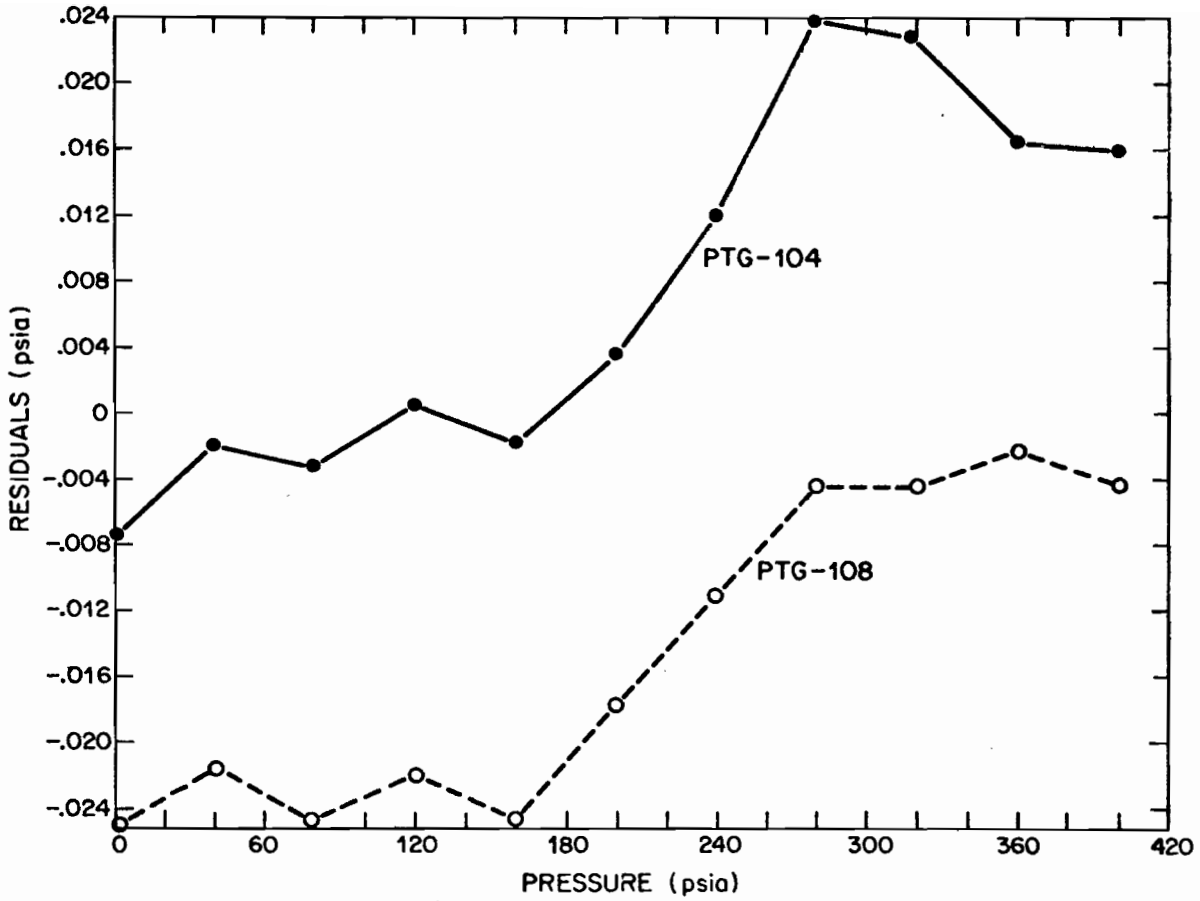

Figure 9. Residuals between applied pressure and calculated pressure. The calculated pressure is based on the calibration curve found during the first emersion (see text).

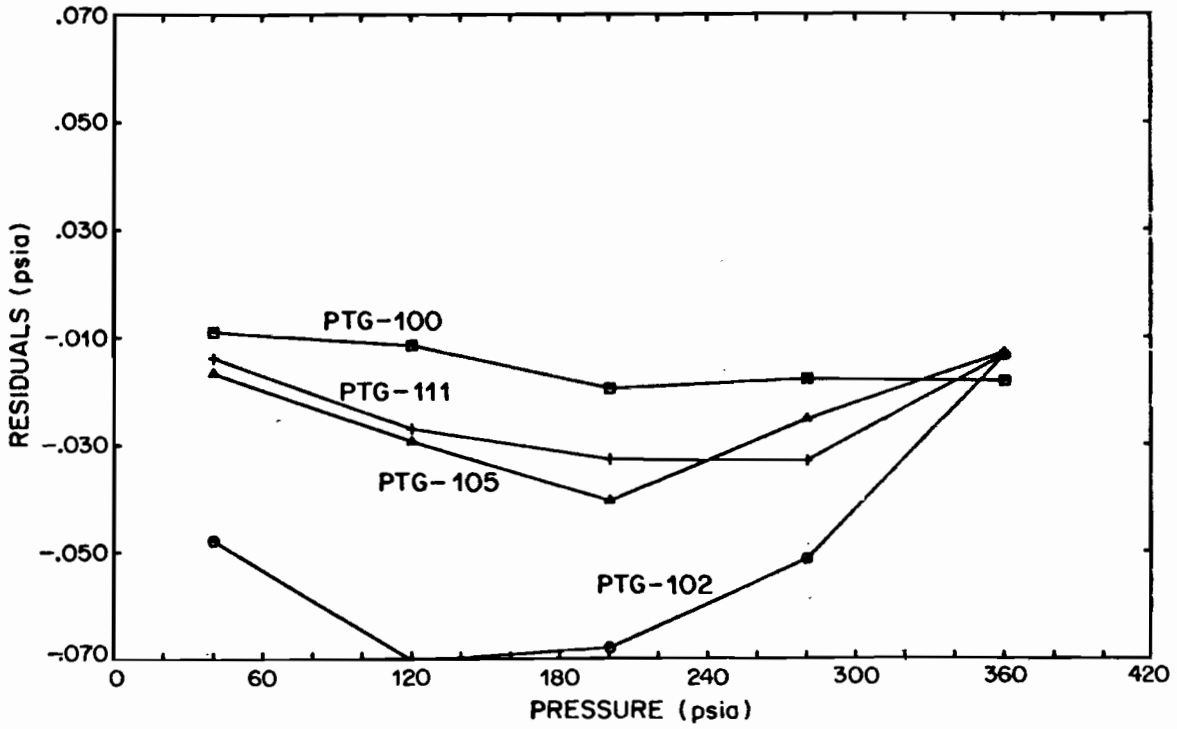

Figure 10. Pressure gage hysteresis. The calculated pressure is based on the calibration curve fit to the data when the pressure was increasing. The residuals shown are between calculated and measured pressure for pressures decreasing.

negligible (i.e., < 0.5 mb). At 100 cm/s the pressure measurements were noisy; however, an average change of 5 mb was observed.

The importance of this effect will depend upon the application of the PTG. For bottom measurements in the Gulf of Alaska the effect is not considered important. Velocities 10 m from the bottom are generally less than 30 cm/s. The velocity 1 m above the bottom (the approximate height of the pressure port) will be less than this. In tidal channels, large flows may be observed and the effect might be important.

4. DATA PROCESSING

4.1 Processing of Data Taken at Sea

The gage writes a three-word record (clock, pressure, temperature) every 900 s onto a four-track cassette tape. The cassette records are transferred to seven-track (computer-compatible) tape with a Sea Data model 12 reader and a Digi-Data Corporation recorder. During this process, the logical structure of the data and the parity are checked. Figure 11 is a flow chart describing the data processing system.

Program TG-1 buffers in seven-track tape record and unpack the bits into clock, pressure, and temperature words. If an error is encountered, its type is indicated by a coded error word. Temperature and pressure words are converted to frequency (i.e., divided by the sample interval of 900 s). Temperature and/or pressure calibration polynomials may be applied if they are available. Program output is on seven-track tape and either microfiche or line printer list. Each output record consists of:

(1) error word
(2) clock word
(3) pressure frequency
(4) temperature frequency
(5) pressure (db) (if calibration coefficients used)
(6) temperature (°C) (if calibration coefficients used)
(7) line count.

The clock word is checked (the clock should increment every 450 s), and records with an improper clock word are visually flagged on the output listing. The output also includes the total number of records encountered, with errors and improper clock words.

A GMT time and date is assigned to every record from the following: (1) pre-deployment clock reset time, (2) pre-deployment and/or post-recovery "events" (i.e., pressure "pump-up" with a hand pump at a known time), and (3) deployment and recovery checkoff sheets.

With this information, basic statistics (mean, standard deviation, variance, skewness, kurtosis, extrema) can be calculated for pressure and

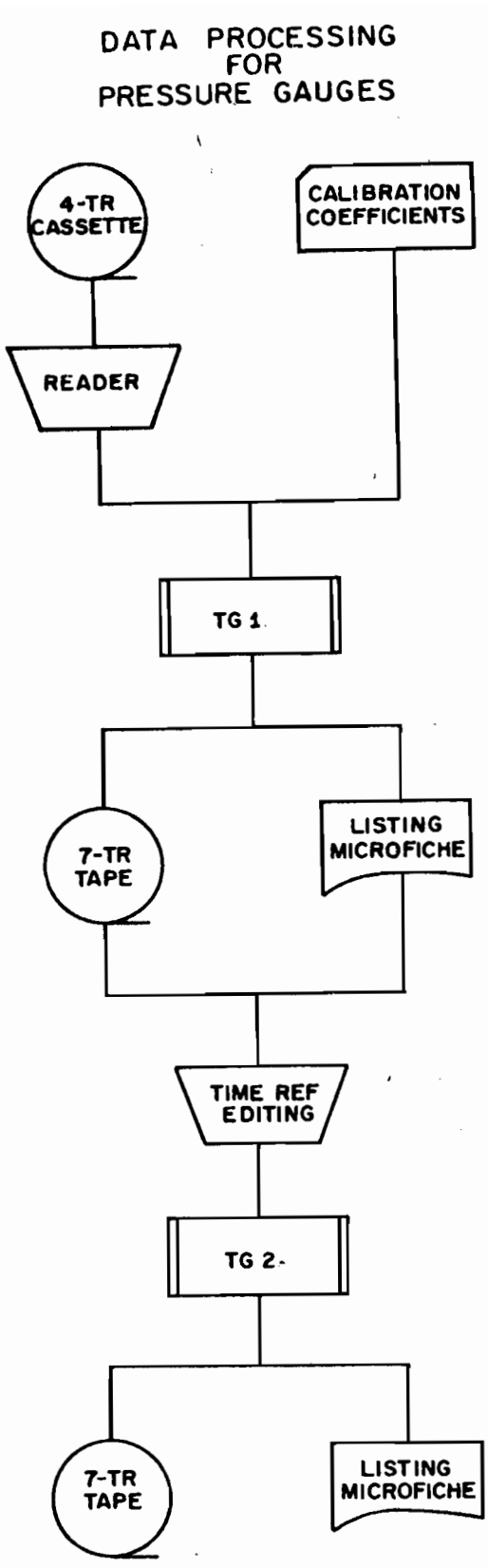

Figure 11. Flow chart of pressure processing programs.

temperature (either frequencies or actual values) during the period of deployment. (Values with bad error words are omitted from calculations.) If the pressure or temperature seems incorrect, the microfiche listing is visually scanned or the data is plotted to locate "bad" points. If the incorrect data are accompanied by error tags, they will be replaced automatically by Program TG2. If not, TG2 has options to permit insertion or replacement of bad values. If many data values are bad, another computer program is used to display the bit patterns of the words in question. If necessary, these patterns can be modified by rerunning program TG1 with temporary modifications.

Program TG2 applies time/date words to each record and replaces, by linear interpolation, any record with an error tag. It has options for editing: (1) inserting data values specified on input, (2) replacing data values specified on input, (3) replacing data records which have temperature or pressure values outside specified limits; and for calibration: (1) applying calibration coefficients for temperature and/or pressure, (2) applying a correction for time dependence of the pressure calibration, and (3) applying a correction for temperature dependence.

Output includes the number of values replaced by editing options, the line count of values outside pressure or temperature windows, the calibration coefficients, and the last data record. The following output values are written on seven-track tape and are optionally listed on microfiche:

(1) time/date (GMT)
(2) pressure (db)
(3) temperature (°C)
(4) line count.

This magnetic tape is used for most of the subsequent plotting and time series data analysis performed with standard programs in the PMEL program library.

4.2 Processing of Calibration Data

Figure 12 is a flow chart of the data processing system for calibration of pressure gages. The cassette tape is translated to a seven-track tape which is read by program TG1, as described in section 4.1.

Program PRCAL calculates the coefficients of the third-order calibration polynomial by the least squares method. Input to this program consists of the seven-track tape generated by program TG1, the calibration pressures applied at NWRCC, the times when they were applied, and the pressure gage clock reset time. PRCAL lists and punches the calibration data (NWRCC-applied pressures and average frequencies). It also plots the residuals of the curve fit and lists the least squares coefficients.

5. SAMPLE RESULTS

As examples of pressure measurements obtained with the PTG, records from four locations in the Northeast Gulf of Alaska are presented. These

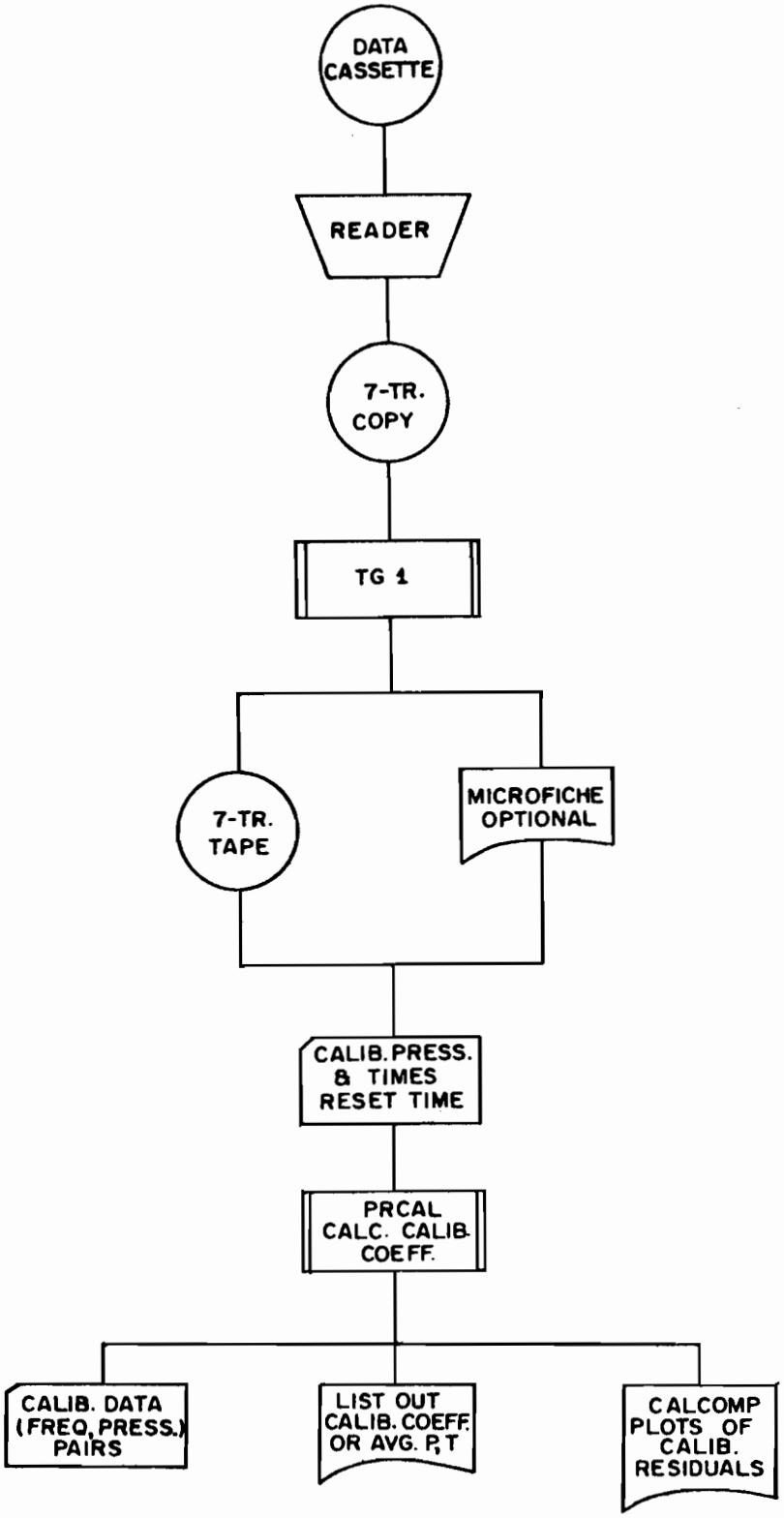

Figure 12. Flow chart of pressure calibration processing programs.

data are discussed more fully in Hayes (1978). A typical mooring diagram is shown in Figure 13. The PTG is clamped to the tension rod of an AMF model 322 acoustic release. This release is attached to a tripod which prevents movement of the PTG and which serves as a platform for the back-up recovery system. The tripod assembly is secured to the railroad wheel anchor via the acoustic release. Upon recovery, the anchor is dropped and the tripod surfaces. The backup recovery unit is a timed release developed at the University of Washington. At a preset time, a float with a tether line is released to the surface to allow retrieval of the anchor and pressure gage assembly in case of primary recovery system failure.

The array location is shown in Figure 14; positions B, C, and D each had a single PTG moored from March 1976 to August 1976. Position A had continuous measurements over this period; however, the gage was changed in May. The nominal depths of the gages were 50 m (B), 100 m (A, C), and 250 m (D). Moorings A and C were about 50 km apart. The array was designed to study the sea level setup caused by alongshore winds.

A portion of the unfiltered data from A and C is shown in Figure 15. The tidal signal dominates. The two series are essentially identical in amplitude and phase. Similar comparison with records from the other locations show near agreement, although there is some modification of the tidal pressure field as the water depth changes.

Figure 16 shows low-pass filtered records from the four locations for the period from March to August. The filter was selected to suppress the diurnal and semidiurnal tides. Mean pressure at each location has been subtracted. The records from A and C have been superimposed to indicate the close agreement between these series. The maximum difference in longshore pressure was about 3 mb. These differences could be caused by real longshore pressure gradients. None of the gages showed a large trend.

Table 1 gives the trend obtained from a least squares linear regression of each series. At the 100-m depth, the trend at both gages is very small. At the 50-m and 100-m locations, the trend was about 1 mb/mo. The agreement of the two gages at the same depth is a good indication that those gages had little or no instrumental drift. However, at the 50-m and 250-m locations, instrumental and oceanic effects cannot be separated.

In general, one would expect the bottom pressure in this region of the Gulf of Alaska to decrease in summer (Hayes and Schumacher, 1976) since the wind setup is reduced, and seasonal heating reduces the water density. The observed trend is in the opposite sense with higher pressures occurring in summer. It is difficult to assess the level of the significance of the trend, since the pressure time series have large energy at low frequencies. Figure 17 shows the 15-day cutoff low-pass filtered records. The observed trend could be associated with these low-frequency oscillations.

Comparison of field data will always yield these ambiguities between instrumental and oceanic effects. However, the overall quality of the

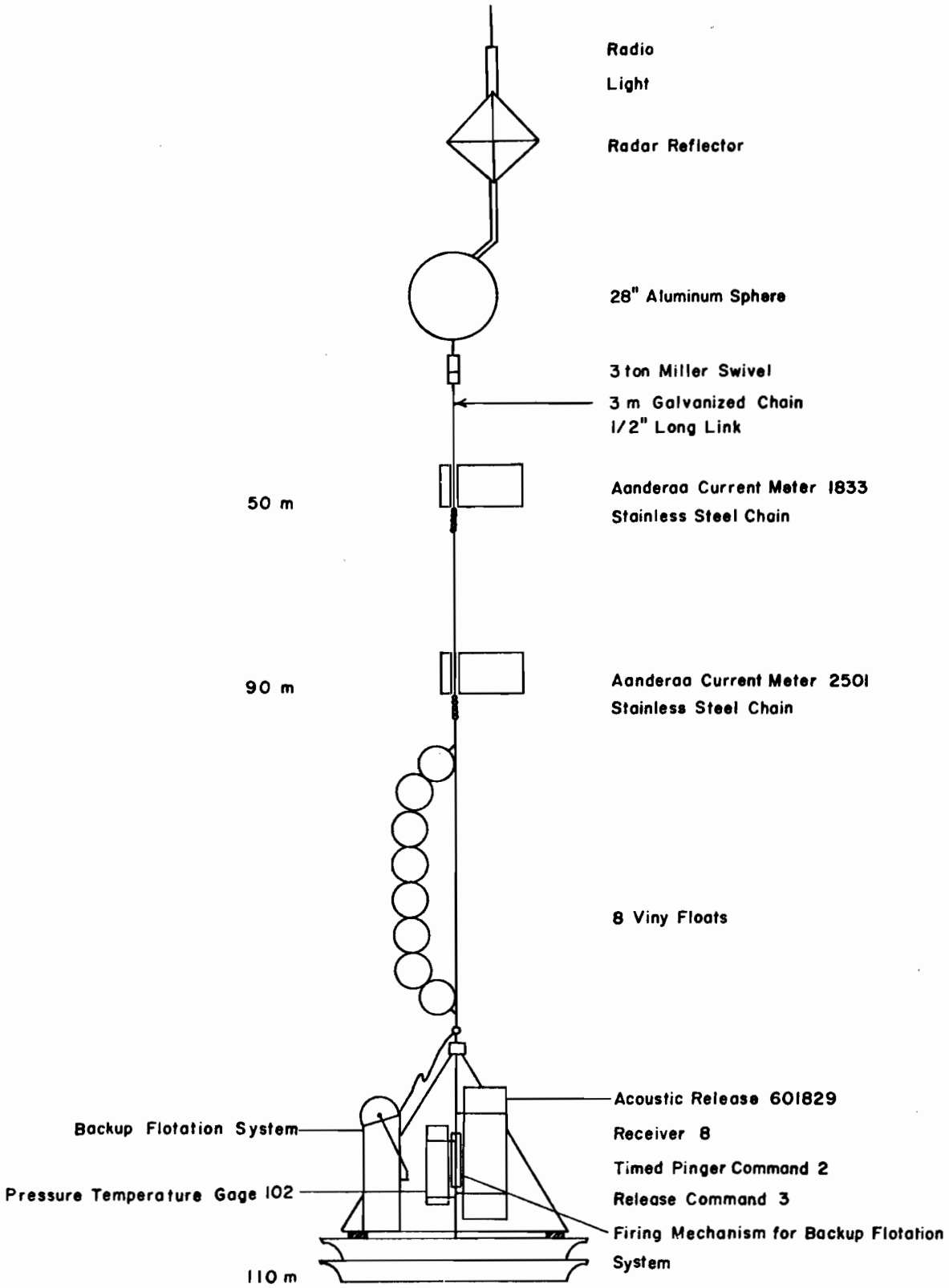

Figure 13. PTG and current meter mooring used in the Gulf of Alaska.

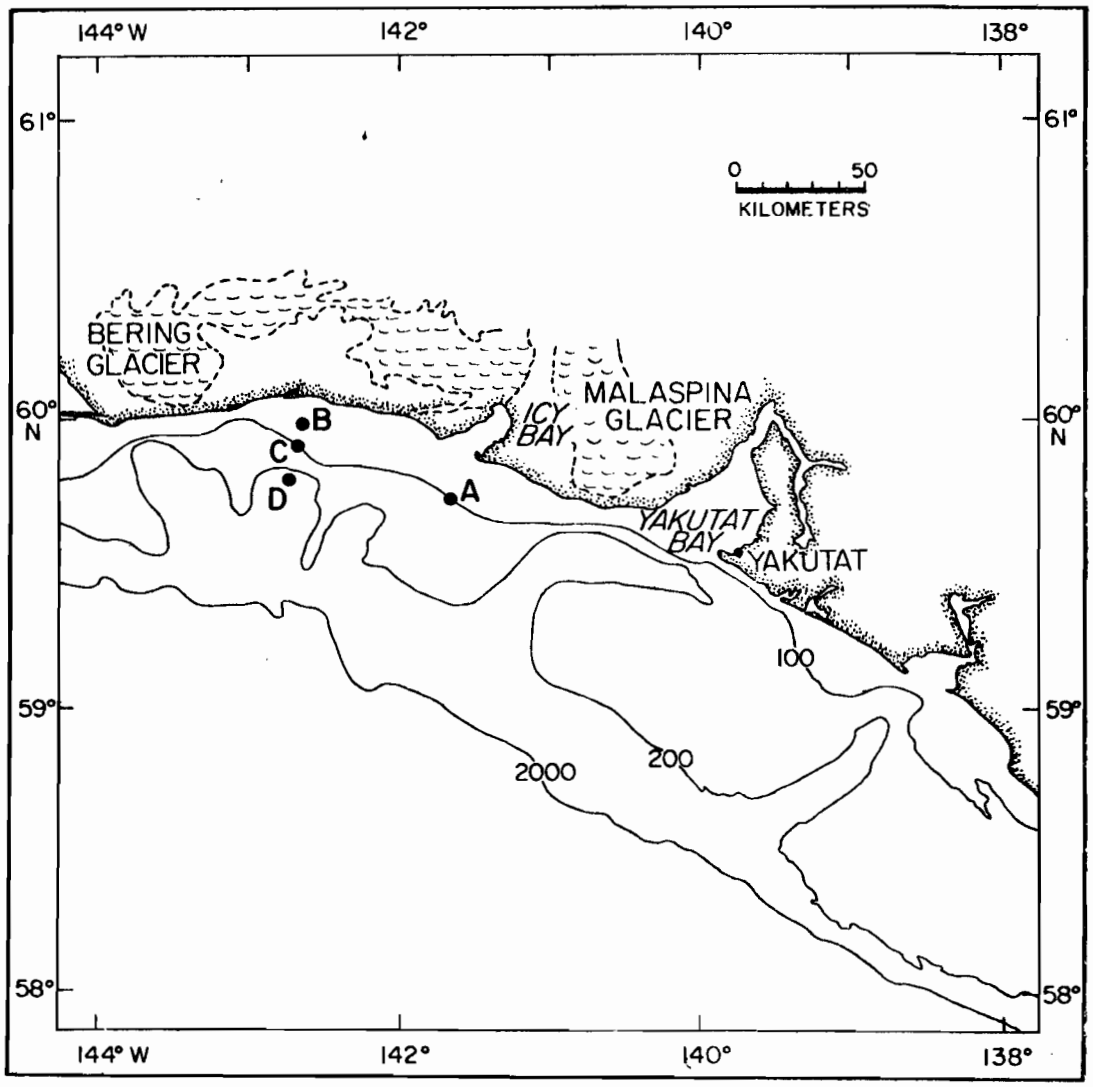

Figure 14. Location of four bottom moored pressure gages in the N.E. Gulf of Alaska.

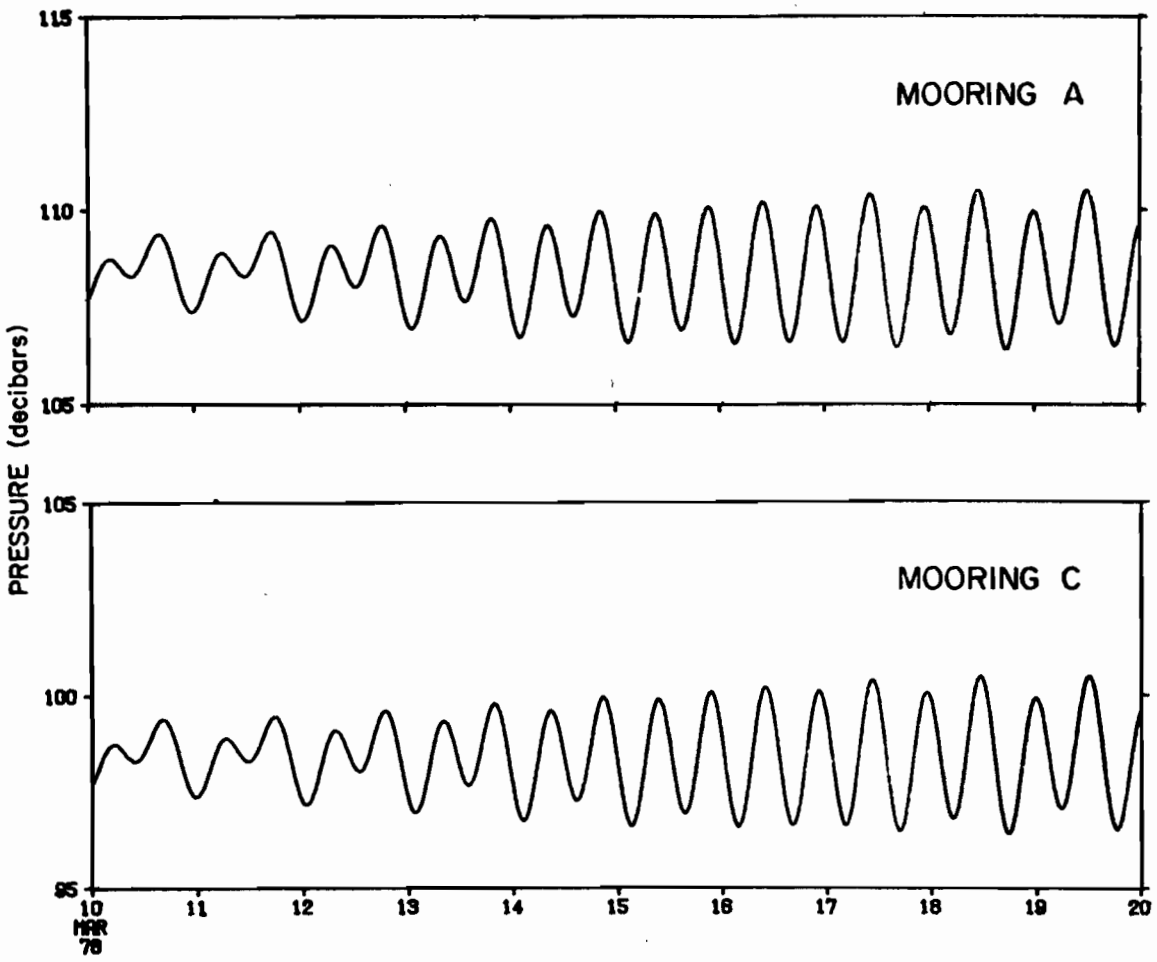

Figure 15. A portion of the unfiltered pressure record at moorings A and C (100 m nominal depth).

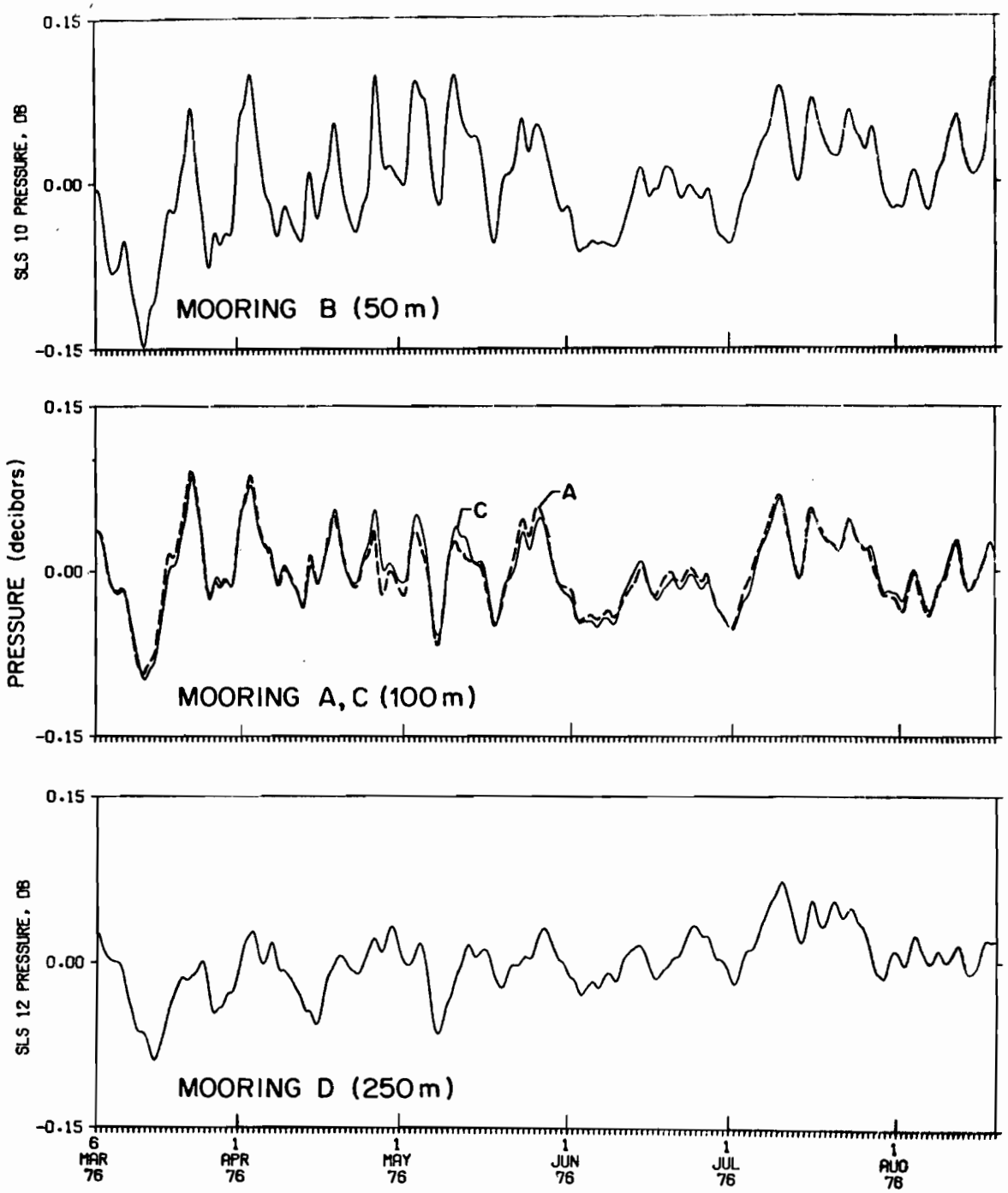

Figure 16. Low pass filtered data at the four locations. The mean of each pressure was removed. Filter cutoff is about 3 days.

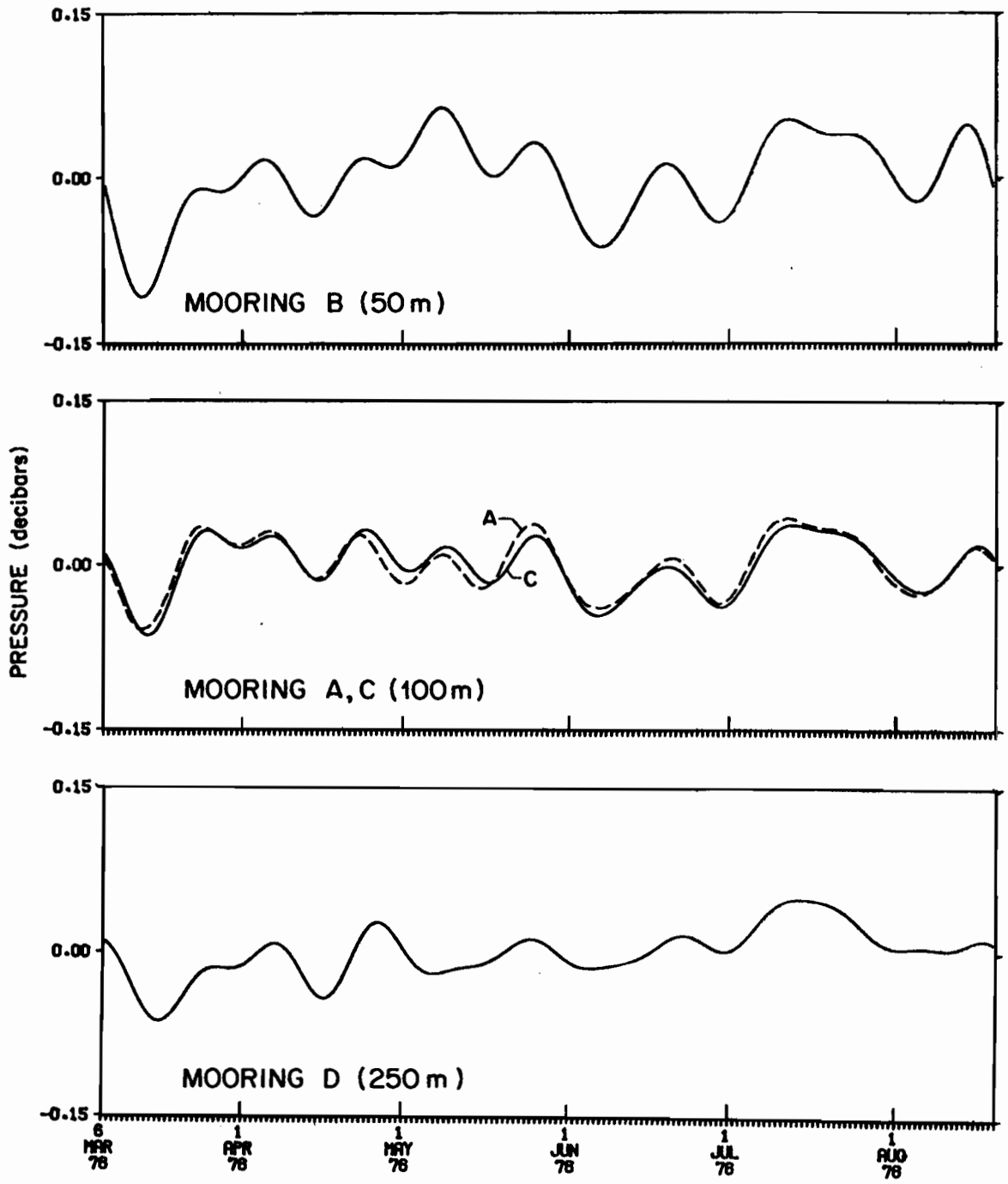

Figure 17. Low pass filtered data at the four locations. Filter cutoff is 15 days.

Table 1. Pressure gage trends from 6 March to 20 August 1976.

Mooring	Depth	Trend
A	100 m	0.04 mb/mo
B	50 m	0.99 mb/mo
C	100 m	0.05 mb/mo
D	250 m	0.93 mb/mo

pressure series and the small trends observed compared to the signals of interest (2- to 10-day storm events) are encouraging. The PTG has proved a valuable research tool for studying ocean dynamics over continental shelves. As additional data is accumulated, we expect to see the use of the gage extended, and new information on instrumental characteristics will be available.

Acknowledgements. We wish to acknowledge the encouragement which D. Halpern gave in the development of this gage. Much of the early design work and prototype development was done by A. M. Zwilling.

The development was supported in part by the Bureau of Land Management through interagency agreement with the National Oceanic and Atmospheric Administration, under which a multi-year program responding to needs of petroleum development of the Alaskan Continental Shelf is managed by the Outer Continental Shelf Environmental Assessment Program (OCSEAP) Office.

6. REFERENCES

Culverhouse, B. (1977): Self-contained digital tide measurement system. NOAA Tech. Memo. ERL AOML-24.

Hayes, S. P. (1978) Variability of current and bottom pressure across the continental shelf in the northeast Gulf of Alaska. J. Phys. Oceanogr. (in press).

Hayes, S. P. and J. D. Schumacher (1976): Description of wind, current, and bottom pressure variations on the continental shelf in the N.E. Gulf of Alaska from February to May 1975. J. Geophys. Res., 18: 6411-6419.

Paros, J. (1976): Digital pressure transducers. Meas. and Data, 10: 74-79.

Steinhart, J. S., and S. R. Hart (1968): Calibration curves for thermistors. Deep-Sea Res., 15:497-503.